J Mater Sci: Mater Med (2008) 19:2293–2299
DOI 10.1007/s10856-007-3333-x

Crystal ageing in irradiated ultra high molecular weight polyethylene

D. Barron · M. N. Collins · M. J. Flannery · J. J. Leahy · C. Birkinshaw

Received: 21 September 2007 / Accepted: 21 November 2007 / Published online: 12 December 2007

Abstract Medical grade ultra high molecular weight polyethylene (UHMWPE) of two molecular weights has been γ irradiated in air to give received doses of 3.5 and 10 Mrad and aged in air for 25 months. Differential scanning calorimetry and wide and small angle X-ray diffraction (WAX and SAX) techniques and transmission electron microscopy have been used to characterize the materials. Polymer from an orthopaedic component, retrieved 10 years after implantation, has been subjected to the same analytical programme. The X-ray diffraction data shows that following irradiation two events occur with time, first a crystal refinement process, indicated by pronounced sharpening of the SAX peak, and secondly growth of a new crystal population of reduced lamellae thickness compared to the original crystal structures, shown by the development of a bimodal SAX pattern. Following irradiation crystallinity increases with time and this second crystal population makes a significant contribution to that increase. The retrieved component shows full development of these processes. It is considered that these crystallographic changes with time are responsible for the observed time dependent changes in the mechanical properties of air irradiated UHMWPE.

1 Introduction

Ultra high molecular weight polyethylene (UHMWPE) is a linear polymer with number average molecular weight values in excess of a million. Crystallinity ranges from 35% to 60%, depending upon grade and thermal history, and crystallinity values are always lower than those recorded for lower molecular weight PE of similar linearity. A combination of hindered molecular diffusion in the melt and the development of inter-lamellae tie chains are responsible for this lower crystallinity and these phenomena are well understood.

Compared with conventional polyethylenes UHMWPE shows much improved creep resistance and this, taken in conjunction with its good abrasion resistance and bio-inertness when in bulk, has encouraged its medical use as a bearing component in replacement joints. For this application it is usual to sterilize the material using γ radiation, with received dose values between 2.5 and 3.5 Mrad. In the past sterilisation was carried out on packaged and sealed materials in air and with air in the package, and this irradiation initiated the high energy photo-oxidation reactions which are again well known with polyolefins. These reactions lead to chain scission, the development of unsaturation, crosslinking and the release of molecular hydrogen. The particular significance of these reactions to UHMWPE is that the scission of inter-lamellae tie chains leads to an immediate increase in crystallinity with consequent increase in modulus and reduction in toughness [1, 2].

It has been demonstrated [3] that very high free radical concentrations persist for many years in irradiated materials. Material irradiated in air initially shows a seven peak electron spin resonance spectrum, and by fitting hyperfine splitting values, and comparison with literature this has been identified as arising primarily from alkyl radicals with smaller contribution from allyl and peroxy radicals. There is some evidence that with time the relative proportion of allyl radicals increases, but comparison of observed and theoretical spectra shows that the allyl radical is less

D. Barron · M. N. Collins · M. J. Flannery · J. J. Leahy · C. Birkinshaw (✉)
Department of Materials Science and Technology, University of Limerick, Limerick, Ireland
e-mail: colin.birkinshaw@ul.ie

significant than the alkyl radical in the first few months of ageing. Photo-oxidative processes and consequent structural rearrangements therefore continue long after the initial sterilization process. Mechanically the material ages, with continuing modulus increase and toughness reduction, with considerable negative consequences for application in orthopaedic components, which have been designed with the original material properties in mind. Examination of retrieved prostheses has shown [4] large strain plastic deformation in the surface material and so morphology analysis is important.

Knowledge of some of these processes has encouraged industrial development of techniques to drive the photo-induced processes towards beneficial crosslinking and away from scission reactions. Methods which have been applied include exclusion of oxygen, thermal annealing and mechanical annealing [5, 6]. However it remains the case that some materials are still irradiated in air and very large numbers of implants are in service having been irradiated in air. The precise nature of the crystal changes that occur on irradiation are therefore of continuing interest and are the focus of this study.

Differential scanning calorimetry (DSC) is traditionally used to measure crystallinity but only provides limited information. In the work described here both wide and small angle X-ray diffraction (WAX and SAX) have been used to provide fundamental crystallographic data on materials before and after irradiation. The use of synchrotron radiation is desirable for SAX experiments and when combined with a heated stage permits melting and recrystallisation of the specimen whilst held in the X-ray beam [7] and allows generation of diffraction contour maps and the calculation of d-spacing and lamella thickness values as a function of temperature. This experimental approach has been developed and applied with success by Ryan and coworkers to polyethylene [8] and polypropylene [9, 10]. Transmission electron microscopy allows visualization of the structures present and assessment of the level of order in the system. Taken together all of this information gives a relatively complete picture of the types of order present in UHMWPE and the effects of sterilizing radiation and ageing.

2 Experimental

Materials used were GUR 1020 and GUR 1050, manufactured by Ticona, and specified to have Mw values of 3.5 and 5.5 million, respectively. Samples, in the form of blocks approximately 10 mm × 10 mm × 50 mm, were irradiated in air using a cobalt 60 source at a rate of 0.15 Mrad per hour to give received dose of 3.5 and 10 Mrad and were analysed within 5 days of irradiation. Ageing was carried out at room temperature in darkness for 25 months. Also evaluated was a retrieved tibial implant, manufactured from the then equivalent material to GUR 1020 and irradiated at a dose level of 2.5 Mrad and implanted 10 years previously. This implant had failed by fracture and had been replaced in a surgical revision procedure.

Differential scanning calorimetry was carried out using a Perkin Elmer Pyris 1, using a sample size of approximately 5 mg and a heating rate of 10 °C per minute under nitrogen. Samples, taken from the centre of the irradiated blocks, were heated to 200 °C, recording the initial melting event and then cooled at 10 °C per minute to record the recrystallisation. A heat of fusion of 291 J/g was used to calculate percentage crystallinity with integration limits determined by inspection and typically being between 118 °C and 148 °C for un-irradiated material.

X-ray diffraction was carried out using the Daresbury, UK, Synchrotron Radiation Source (SRS) beam line number MPW 6.2, described in detail elsewhere [11]. The configuration used allowed synchronised SAXS and WAXS measurements to be made. The SAX camera length was 3.5 m. The standard energy of 8.865 keV (1.40 Å) was used. A Linkam hot stage system was mounted in the beam and was programmed to heat and cool the sample at 10 °C per minute giving a similar melting and cooling regime to that used for DSC. The programming and synchronization of the heated stage and the output from the two one-dimensional rapid response detectors was achieved via SRS in-house software. Analysis of data was carried out using the Bragg equation and in part using software developed by the Collaborative Computational Project for Fibre Diffraction and Solution Scattering (CCP13).

Attempts were made with the assistance of the Rubber and Plastics Research Association to measure, using high temperature size exclusion chromatography, the molecular weights of the materials investigated. A combination of the difficulties of dissolution of very high molecular weight partially crosslinked polymer and simultaneous in-solution oxidation meant that this work was not productive.

Transmission electron microscopy was carried out using a Hitachi instrument. Thin slices were stained using 99% chlorosulphonic acid for 6 h at 60 °C, embedded in epoxy resin and ultra-microtomed to give 40 nm slices which were collected on copper grids and examined at magnifications from 8,000 to 20,000 times.

3 Results

Figure 1 shows the DSC results for the various materials and Table 1 gives the calculated crystallinity values and event temperatures. Figure 2 shows the SAX

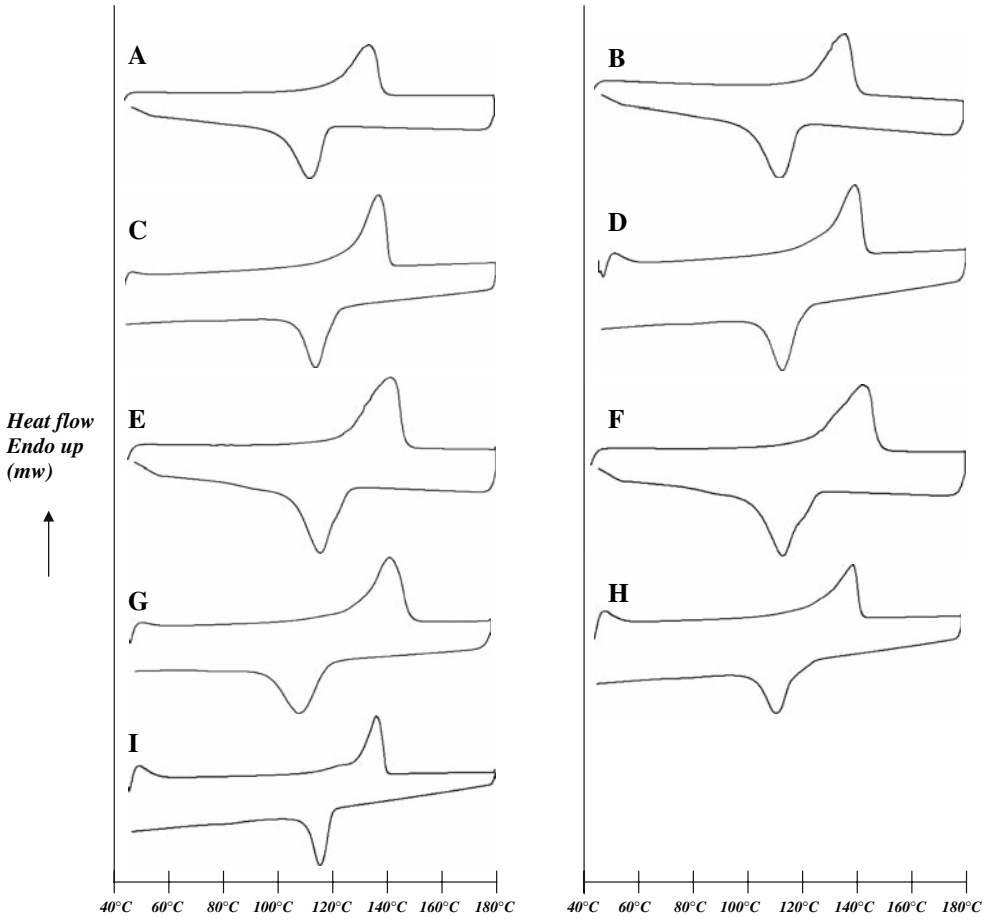

Fig. 1 DSC results for the various materials. (**A**) Control 1020, (**B**) control 1050, (**C**) 1020 3.5 Mrad after 1 week, (**D**) 1050 3.5 Mrad after 1 week, (**E**) 1020 10 Mrad after 1 week, (**F**) 1050 10 Mrad after 1 week, (**G**) 1020 10 Mrad after 25 months, (**H**) 1050 10 Mrad after 25 months, (**I**) 1020 retrieved sample

plots as the sample is heated through melting, and then cooled and crystallized. Table 2 details the lamella thickness at the start and finish of each experiment for all of the materials. Figure 3 shows the WAX and SAX contour plots for the unirradiated GUR 1020 material. Figure 4 shows the equivalent data for the retrieved implant. Figures 5 and 6 show transmission electron micrographs of the unirradiated GUR 1020 and the retrieved implant.

4 Discussion

Considering the DSC crystallinity results first, the relationship between the lower and higher molecular weight materials is as expected and is consistent with hindrance to diffusion in the melt. As usual with these materials melting and recrystallisation are broad events and considerable super-cooling is apparent. Just detectable on the low temperature side of the re-crystallisation peaks in the aged

Table 1 Crystallinity values and event temperatures for all of the materials investigated

Condition	1020 Crystallinity (%)	1020 Melting peak (°C)	1020 Crystallisation peak (°C)	1050 Crystallinity (%)	1050 Melting peak (°C)	1050 Crystallisation peak (°C)
Unirradiated	51.6	–	–	45.0	–	–
3.5 Mrad tested after 1 week	58.8	138	118	53.6	141	117
10 Mrad tested after 1 week	57.3	147	117	53.7	146	116
1020 10 Mrad tested after 25 months	60.3	146	110	51.7	140	114
1020 Retrieved 10 years old implant material	70.0	138	118	–	–	–

All results are the average of three determinations

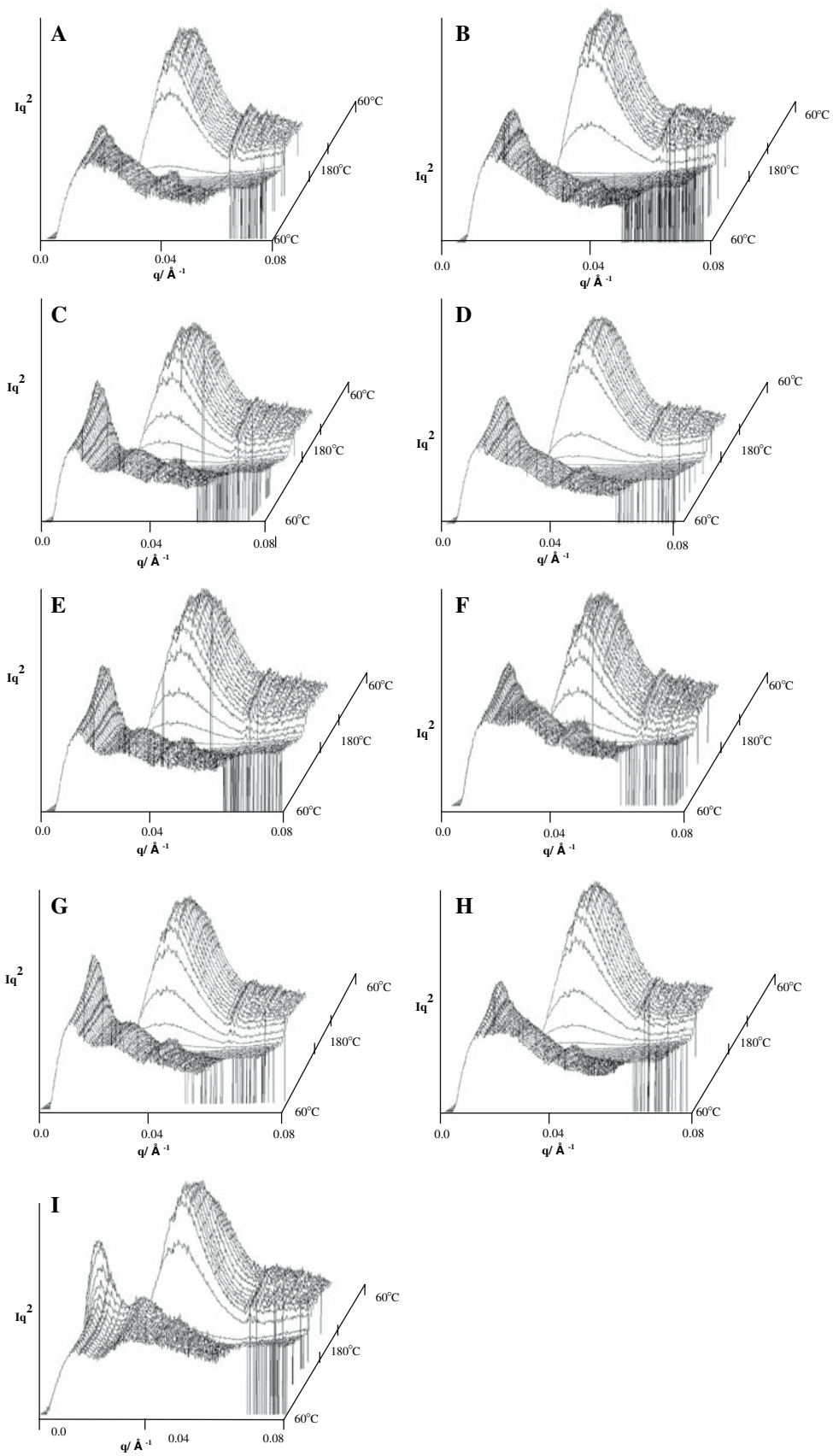

Fig. 2 SAX plots for melting and recrystallisation. Heating and cooling rate 10 °C per minute. (**A**) 1020 Unirradiated, (**B**) 1050 unirradiated, (**C**) 1020 3.5 Mrad tested after 1 week, (**D**) 1050 3.5 Mrad tested after 1 week, (**E**) 1020 10 Mrad tested after 1 week, (**F**) 1050 10 Mrad tested after 1 week, (**G**) 1020 10 Mrad tested after 25 months, (**H**) 1050 10 Mrad tested after 25 months, (**I**) 1020 retrieved 10 years old implant material

Table 2 Lamella thickness at the start and finish of each experiment for all of the materials investigated

Condition	1020 Lamella thickness before melting (A)	1020 Lamella thickness following re-crystallisation (A)	1050 Lamella thickness before melting (A)	1050 Lamella thickness following re-crystallisation (A)
Unirradiradiated	182	83	135	103
3.5 Mrad tested after 1 week	140	64	164	91
10 Mrad tested after 1 week	156	82	193	84
10 Mrad tested after 25 months	223	110	138	80
1020 Retrieved 10 years old implant material	192	105	–	–

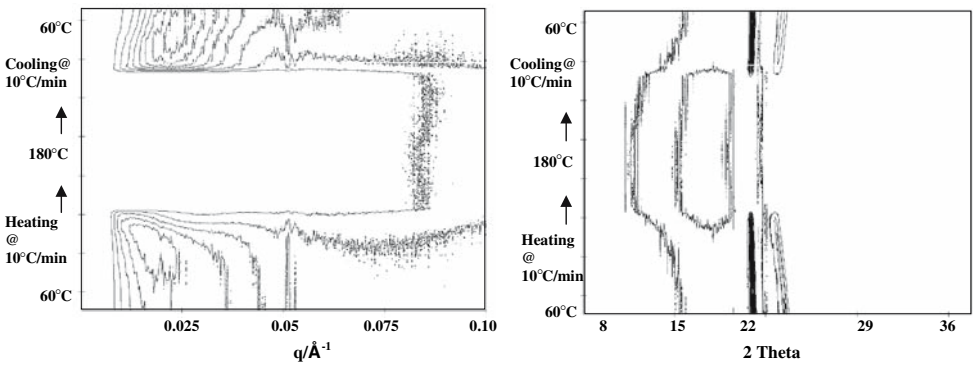

Fig. 3 SAX and WAX contour plots for unirradiated GUR 1020

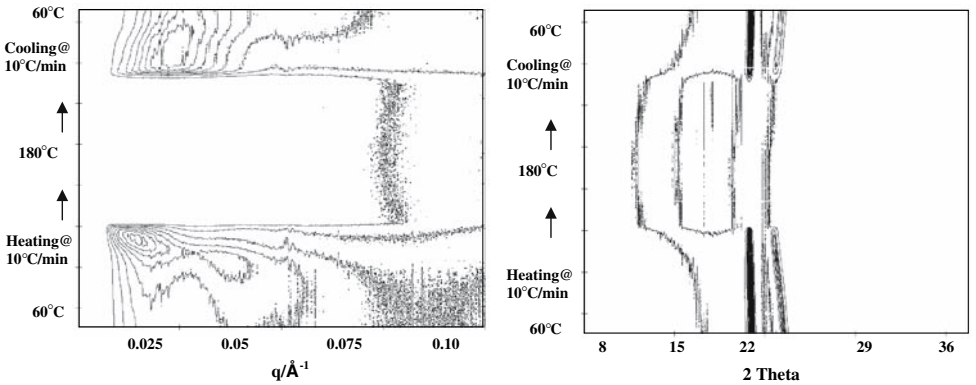

Fig. 4 SAX and WAX contour plots for 10-year-old retrieved implant material

materials is a secondary crystallisation event and following on previous isothermal crystallisation experiments [12] it has been proposed that this is associated with ordering processes in the crystal-amorphous interfacial region. Ageing shows a general trend towards increasing crystallinity, although the value obtained after 25 months with the 1050 material is lower than expected. A difficulty in measuring crystallinity with these materials is the existence of oxidation gradients [13] leading to significant crystallinity variation within a component. Although all results reported here are from the bulk, as opposed to the surface, such effects are difficult to avoid.

The retrieved component shows a sharper DSC profile and an extremely high crystal content of 70%. Also evident is a secondary melting event as well as the previously mentioned secondary re-crystallisation event.

The peaks evident in the WAX patterns (*110, 200 and 210* planes) have been indexed and according to the literature [14, 15] are those of the orthorhombic crystal structure as found in lower molecular weight fractions of polyethylene. The lattice expansion with temperature (particularly evident for the *200* plane) seen in the contour plot shown as Fig. 3, and typical of all of the materials examined, is consistent with the observations of others [15]. The final collapse of the lattice is quite abrupt, occurring at 145 °C and is associated with the breakdown of the most perfect crystallites present.

Once again significant supercooling can be seen on re-crystallisation and is similar to that observed in the DSC experiments. It is also apparent that the lattice parameters are slightly altered by the recrystallisation process. This may be a function of heating rate differences between the

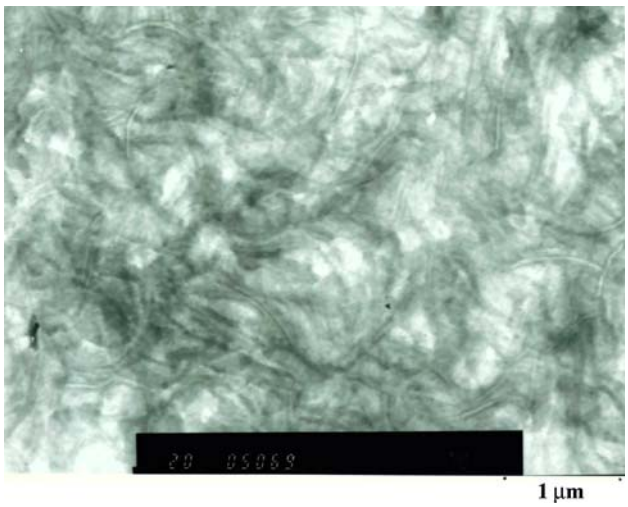

Fig. 5 Transmission electron micrograph of unirradiated 1020 material

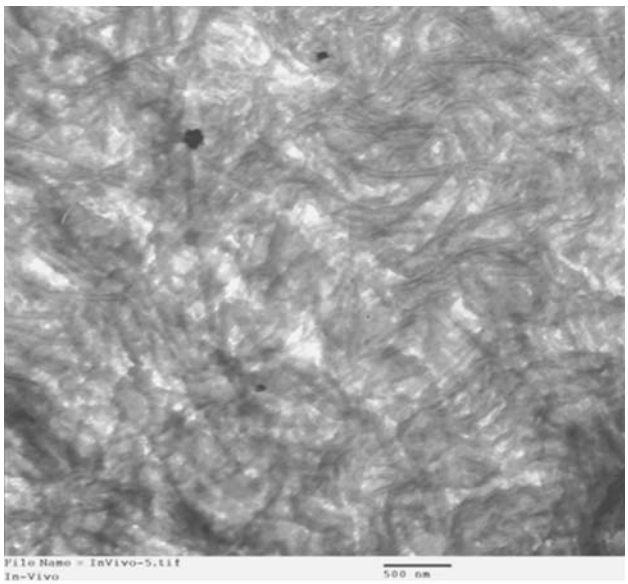

Fig. 6 Transmission electron micrograph of material from the retrieved implant

original crystallisation conditions and this experiment, or may arise because of distortions introduced by thermal and photo-oxidation of the sample during the experiment, although this might be expected to influence lamella thickness rather than lattice parameters.

The SAX patterns are characterised by large broad peaks both before and after recrystallisation. It is thought that the small sharp peaks at higher q values are artefacts, but their origin is not known. Lamellae thickness, both before and after recrystallisation is such that the upper edge of the peaks is only just resolved by the 3.5 m camera. Comparison of diffraction data for the lower and higher molecular weight materials before irradiation shows little qualitative difference, as the differences in intensity can be ascribed to the effective sample size exposed to the beam.

Quantitative analysis of the small angle data allows calculation of d-spacing and assuming a two phase model (discussed later) the average lamellar thickness is given by the product of the degree of crystallinity and the d-spacing. A choice exits as to which percentage crytallinity data (WAX or DSC) to use for this calculation, and as it is considered that the DSC integration is less subjective, that data was used here. Percentage crystallinity from WAX data was always much lower than that obtained by DSC. Figures 3 and 4 show how d-spacing and lamella thickness change throughout the melting and re-crystallisation experiment for unirradiated GUR 1020 and the retrieved material. It is appreciated that the assumption that the average lamellar thickness is the product of d-spacing (from SAXS) and degree of crystallinity may not be always correct. SAXS can indicate the d-spacing within crystalline stacks, while the degree of crystallinity by DSC also depends on amorphous material outside of the crystalline stacks.

Given the limitations to synchrotron beam-line time these are of necessity single experiments, however considering the results in Table 2, the lamella thickness of the original lower molecular weight material is seen to be around 182 A, indicating approximately 118 repeat units per fold length. The higher molecular weight material is slightly less than this at about 135 A indicating about 88 repeat units per fold length. Re-crystallisation always leads to thinner lamellae and this is probably a cooling rate effect. The original materials were taken from large compression moulded blocks and therefore subject to much slower cooling rates than the 10 °C per minute used in the synchrotron re-crystallisation experiments. Taken overall there is little change in lamellae thickness with dose or with ageing, indicating that the system is close to the optimum fold width for the particular cooling conditions.

However there are two striking observations in the SAX patterns. First, with irradiation and ageing the peaks show appreciable sharpening indicative of a crystal refinement process, and secondly the development of a second diffraction peak at higher q-values than the main peak, and therefore associated with smaller structures. Presumably the lamellae thicknesses of the new smaller crystals is not a simple fraction of the thickness of the original crystals. This bi-modal SAX pattern is particularly evident with the GUR 1020 series of results and with the retrieved component.

It is presumed that the processes at work here are initiated by chain scission within the amorphous phase and that two paths are followed, one leading to the refining of the original lamellae and the other to the formation of a sub-population of smaller crystals. Prenmath et al. [16]

have also suggested that irradiation and ageing leads to the formation of thin crystallites within the amorphous region. At room temperature the polymer is mid-way between T_g and T_m and so reorganisation can be expected to be rapid if constraints such as inter-lamellae tie chains are removed. It is possible that a significant proportion of the folds within the lamellae do not involve immediate re-entry of the chain and scission of loops as well as tie chains will make new material available for folding. Evidence exists [17, 18] for the presence of a substantial semi-ordered interfacial phase in polyethylenes and experimental observation has shown [19] that UHMWPE also possesses a significant inter-facial phase. Scission within this phase can be expected to account for tidying up of the fold surfaces and a considerable degree of crystal refinement. The growth of the second crystal population, also evident in the DSC melting of the retrieved polymer, is presumed to arise from released material that is too distant from the original lamellae or is somehow prevented by steric factors from taking part in the previously described process. It could be expected that crystallisation should drive this secondary crystallisation towards the thermodynamic optimum lamella thickness but perhaps cross-linking within the amorphous phase prevents this from being achieved. It seems probable that this second crystal population makes a significant contribution to the overall crystallinity increase on ageing.

The electron micrographs shown the extreme tortuosity of the lamellae in both original and aged irradiated materials. There is no evidence, in any case, of crystal association structures such as spherulites. Optical estimation of the lamellae thickness from the images shown in Figs. 5 and 6 suggest values in the range 40–50 nm, values much higher than those obtained by SAX analysis, illustrating the difficulty of comparing crystallographic data obtained using different techniques. Perhaps the larger dimension from SEM measurement arises because of a contribution from the interfacial material, which shows a similar staining response to the true crystals.

5 Conclusions

Crystal ageing within irradiated UHMWPE is associated with a lamellae refinement, indicated by sharpening of the SAX diffraction patterns, and growth of a second population of smaller crystals, shown by development of bimodality in the SAX patterns. Lamellae thickness of the original crystal structures changes little with age and the increase in crystallinity on ageing is largely associated with the growth of the second crystal population. Examination of retrieved material shows the full development of these crystal ageing processes. It is considered that these processes, arising from photo-oxidative chain scission and cross-linking are responsible for the well-known time dependent effects observed with irradiated UHMWPE.

Acknowledgments This work was made possible by a grant of time on the MPW 6.2 station of the Daresbury SRS for which the authors are grateful. The authors also wish to express their thanks to Dr. Chris Martin for his invaluable assistance in setting up the beamline for the experiments.

References

1. C. BIRKINSHAW, M. BUGGY, and J. J. WHITE, *Mater. Chem. Phys.* **14** (1986) 549
2. C. BIRKINSHAW, M. BUGGY, S. DALY, and M. O'NEILL, *Polym. Degrad. Stabil.* **22** (1988) 285
3. P. O'NEILL, C. BIRKINSHAW, J. J. LEAHY, and R. BARKLEY, *Polym. Degrad. Stabil.* **63** (1999) 31
4. M. JASTY, D. D. GOETZ, C. R. BRAGDON, K. R. LEE, A. E. HANSON, J. R. ELDER, and W. H. HARRIS, *J. Bone Joint Surg.-Am.* **79A** (1997) 349
5. J. H. DUMBLETON, J. A. D'ANTONIO, M. T. MANLEY, W. N. CAPELLO, and A. WANG, *Clin. Orthop. Relat. Res.* **453** (2006) 265
6. A. WANG, H. ZENG, S. S. YAU, A. ESSNER, M. MANLEY, and J. DUMBLETON, *J. Phys. D-Appl. Phys.* **39** (2006) 3213
7. W. BRAS, G. DERBYSHIRE, A. RYAN, G. MANT, R. LEWIS, A. FELTON, and N. GREAVES, *Inst. Phys. Conf. Ser.* **130** (1993) 635
8. A. RYAN, W. BRAS, G. R. MANT, and G. E. DERBYSHIRE, *Polymer* **35** (1994) 4537
9. W. J. O'KANE, R. J. YOUNG, A. J. RYAN, W. BRAS, G. E. DERBYSHIRE, and G.R. MANT, *Polymer* **35** (1994) 1352
10. E. L. HEELEY, A. V. MAIDENS, P. D. OLMSTED, W. BRAS, I. P. DOLBNYA, J. P. A. FAIRCLOUGH, N. J. TERRILL, and A. J. RYAN, *Macromolecules* **36** (2003) 3656
11. R. J. CERNIK, P. BARNES, G. BUSHNELL-WYE, A. J. DENT, G. P. DIAKUN, J. V. FLAHERTY, G. N. GREAVES, E. L. HEELEY, W. HELSBY, S. D. M. JACQUES, J. KAY. T. RAYMENT, A. RYAN, C. C. TANG, and N. J. TERRILL, *J. Synchrotron Radiat.* **11** (2004) 163
12. D. BARRON and C. BIRKINSHAW, *Polymer* **46** (2005) 9523
13. P. O'NEILL, C. BIRKINSHAW, J. J. LEAHY, M. BUGGY, and T. ASHIDA, *Polym. Degrad. Stabil.* **49** (1995) 239
14. L. H. SPERLING, in "Introduction to Physical Polymer Science" (John Wiley & Sons, New York, 1986)
15. F. J. BALTA-CALLEJA and C. G. VONK, in "X-ray Scattering of Synthetic Polymers" (Elsevier, New York, 1989)
16. V. PRENMATH, A. BELLARE, E. W. MERRILL, M. JASTY, and W. H. HARRIS, *Polymer* **40** (1999) 2215
17. G. R. STROBL and W. HAGEDORN, *J. Polym. Sci. Part B-Polym. Phys.* **16** (1978) 1181
18. R. MUTTER, W. STILLE, and G. STROBL, *J. Polym. Sci. B: Polym. Phys.* **31** (1993) 99
19. D. BARRON, in "The Morphology of Irradiated Ultra High Molecular Weight Polyethylenes". PhD thesis, (University of Limerick, 2007)